# Stochastic ion acceleration by beating electrostatic waves

B. Jorns and E. Y. Choueiri
*Electric Propulsion and Plasma Dynamics Laboratory (EPPDyL), Princeton University, Princeton, New Jersey 08544, USA*
(Received 4 October 2012; published 23 January 2013)

A study is presented of the stochasticity in the orbit of a single, magnetized ion produced by the particle's interaction with two beating electrostatic waves whose frequencies differ by the ion cyclotron frequency. A second-order Lie transform perturbation theory is employed in conjunction with a numerical analysis of the maximum Lyapunov exponent to determine the velocity conditions under which stochasticity occurs in this dynamical system. Upper and lower bounds in ion velocity are found for stochastic orbits with the lower bound approximately equal to the phase velocity of the slower wave. A threshold condition for the onset of stochasticity that is linear with respect to the wave amplitudes is also derived. It is shown that the onset of stochasticity occurs for beating electrostatic waves at lower total wave energy densities than for the case of a single electrostatic wave or two nonbeating electrostatic waves.

DOI: 10.1103/PhysRevE.87.013107 PACS number(s): 52.35.Mw, 52.50.Qt, 02.50.Ey, 45.10.Hj

## I. INTRODUCTION

The ability of electrostatic waves to heat and directly accelerate the charged particles of a magnetized plasma makes them attractive candidates for applications in both industry and research. A large body of work accordingly has been devoted to understanding electrostatic wave-particle interactions. Many of these investigations have focused on a theoretical and experimental characterization of the traditional quasilinear interactions (Landau and cyclotron damping), while for increasing wave amplitude, nonlinear effects such as particle trapping, higher-order wave-wave interactions, and the decorrelation of particle orbits also have been identified (cf. Refs. [1,2]). This last process, which we denote the single electrostatic wave (SEW) interaction, is of particular interest since it provides a mechanism for efficient energy deposition that persists even for nearly perpendicularly propagating modes. This ability stems from the onset of stochasticity in the particle cyclotron orbits due to the presence of a large-amplitude wave [3].

Theoretical and numerical studies of the SEW process have revealed that while the onset of stochasticity depends on nonlinear effects, the energy-exchange with ions is approximately a resonant process [4,5] where only particles with velocities close to the phase velocity of the wave are subject to stochastic acceleration. This resonant requirement for acceleration can significantly limit the energization of particles in low-temperature plasmas where only a few particles are close to the wave-phase velocity. Increasing the amplitude of the wave can in part circumvent this difficulty by expanding the resonant condition to a range around the phase velocity of the wave [3]. However, for a particularly strong perturbation, self-consistent, nonlinear effects such as particle trapping limit the wave amplitude and thereby reduce the efficacy of the SEW interaction.

It is possible to avoid this resonant condition by employing two electrostatic waves in the magnetized plasma. From a single-ion description it has been demonstrated that when two waves satisfy the so-called beat criterion, $\omega_2 - \omega_1 = n\Omega$, where $\omega_1, \omega_2$ are the wave frequencies, $\Omega$ is the ion cyclotron frequency, and $n$ is an integer, ions with initial velocity below the SEW phase velocity can experience significant acceleration through a two-stage process. First, the ions are coherently accelerated by the slowly varying beat envelope at the difference frequency $\omega_2 - \omega_1$ of the beating electrostatic waves (BEW). Second, after these ions have been accelerated to the phase velocities of the individual BEW, the much faster stochastic effects characteristic of SEW dominate and ions are accelerated even further through a random walk in velocity space. The net result of this effect is that even low-temperature distributions with the majority of ions with velocities well below the resonant condition can be significantly energized by the BEW.

The coherent acceleration of the low-energy ions characteristic of the two-stage BEW process has been the subject of a number of theoretical and numerical studies [6–13]. These investigations have not only predicted analytically the orbits followed by the low-energy and coherently accelerated ions subject to BEW [8–10] but also—for a special case of wave parameters—the necessary and sufficient conditions for this acceleration to occur [11].

Most of these single-ion results are valid only for velocities below the SEW resonant conditions of each wave, however, and with the exception of a first-order on-resonance analysis done by Benisti [9] and a numerical argument presented by Sheng [12], the full extent of acceleration for ions after they reach this resonant condition is unknown. Indeed, the stochastic acceleration produced by BEW is not well understood, and to date it simply has been assumed without proof that these high-energy orbits follow the well-established trends of stochasticity for SEW ion acceleration [8,10,13]. This is a critical oversight given the twofold importance of stochastic effects to the BEW acceleration process. First, without decorrelation of particle orbits to supplement the coherent acceleration provided by BEW, the increase in ion energy can be significantly limited [6,9]. Second, in addition to the coherent acceleration provided by the BEW, the existence of the beat resonance between the two waves suggests that for equal wave energy density, the onset of stochasticity for BEW should be lower than the SEW case [12]. Enhanced particle heating therefore should be expected for lower input energy with the BEW case—even when the coherent beat effect is supressed (when collisionality, for example, is dominant).

 

Stochasticity is, thus, an important consideration for the BEW process, and the need is apparent for a systematic evaluation of this effect. The goal of this investigation is to achieve this end by deriving an expression that indicates three critical aspects of the stochasticity: the threshold wave amplitudes for the onset of stochasticity, the lower bound in ion velocity at which this stochastic effect occurs, and the upper bound in ion velocity for particles subject to stochasticity.

In the following section, we begin with the case of perpendicular propagation and review the relevant equations of motion for the interaction of a single ion with BEW. In the third part, we examine analytically and numerically the particle dynamics through the use of the Poincaré cross section. We also demonstrate in that section trends for the onset of stochasticity and its boundaries in phase space. In the fourth section, we derive an analytical condition for the onset of stochasticity, which we subsequently verify numerically in the following section through an analysis of the maximum Lyapunov exponents. For the sixth part, we use our analytically derived condition to compare the onset of stochasticity for the SEW, BEW, and two nonbeating waves. In the last section, we extend our results from the perpendicularly propagating case to allow for a finite parallel wave number and derive a modified form of the stochasticity parameter.

## II. EQUATIONS OF MOTIONS

The equation of motion for a charged particle subject to two perpendicularly propagating electrostatic waves in a uniform magnetic field is given by [10]

$$m\frac{d^2\mathbf{x}}{dt^2} = q\sum_{i=1}^{2}\Phi_i k_i \sin(k_i x - \omega_i t + \varphi_i)\hat{x} + q\mathbf{v}\times\mathbf{B}_0, \qquad (1)$$

where $m$ denotes the ion mass, $q$ is the charge, $\Phi_i$ is the potential amplitude, $k_i$ is the wave vector where we have denoted the direction of propagation as $\hat{x}$, $\omega_i$ is the wave frequency, $\mathbf{B}_0 = B_0\hat{z}$ denotes the background magnetic field, and $\varphi_i$ is the phase of the wave.

We can express these dynamics in a normalized, action-angle formulation that is more easily analyzed by perturbation methods [10]. This yields

$$H = I + \sum_{i=1}^{2}\varepsilon_i \cos(\kappa_i \rho \sin\theta - \nu_i \tau + \varphi_i), \qquad (2)$$

where capitalized letters denote normalized quantities, $I = \frac{1}{2}(V_x^2 + V_y^2)$ is the kinetic energy of the particle, $\nu_i = \omega_i/\Omega$, $\rho = \sqrt{2I}$, $\varepsilon_i = (qk_1^2\Phi_i/m\Omega^2)$ where $\Omega$ is the cyclotron frequency, $\kappa_i = k_i/k_1$, $\theta$ is the angle of cyclotron precession measured from the $x$ direction, and $\tau = t\Omega$. In this system, lengths have been normalized by the wavelength $k_1^{-1}$ and velocities have been normalized by the term $\Omega/k_1$.

It should be noted that in this formulation, the definition of the normalized wave amplitude $\varepsilon_i$ differs from those in related references [8,11] by a factor of $k_1/\Omega$. This stems from our anticipated need to accommodate obliquely propagating waves with respect to the background magnetic field. Further implicit in this derivation is the result that the guiding center of motion in the $\hat{x}$ direction is a constant of motion. This allows for the elimination of a degree of freedom in the problem—as has been done in Eq. (2).

We now see that the equations of motion can easily be separated into an action $H_0 = I$ that is modified by a phase- and time-dependent term $H_1(I,\theta,\tau)$. This form lends itself to perturbation analysis techniques that we employ in different measure throughout our investigation. Specifically, we can express Eq. (2) in a more tractable form by employing a second-order (in amplitudes $\varepsilon_1,\varepsilon_2$) canonical transformation that was derived with the method of Lie transforms in Ref. [8],

$$\tilde{H} = I + \sum_{i=1}^{2}\varepsilon_i^2 S_1^{\nu_i}(\tilde{\rho}) + \varepsilon_1\varepsilon_2\cos[(\nu_1-\nu_2)(\tilde{\theta}-\tau)+\varphi_1-\varphi_2]S_6(\tilde{\rho}), \qquad (3)$$

where

$$S_1^{\nu_i}(\tilde{\rho}) = \sum_m \frac{mJ_m(\kappa_i\tilde{\rho})J_m'(\kappa_i\tilde{\rho})}{2\tilde{\rho}(\nu_i - m)}$$

$$S_6(\tilde{\rho}) = \sum_m \frac{mJ_m(\kappa_1\tilde{\rho})J_{m+1}'(\kappa_2\tilde{\rho})}{2\tilde{\rho}(\nu_1 - m)} + \frac{mJ_m(\kappa_2\tilde{\rho})J_{m-1}'(\kappa_1\tilde{\rho})}{2\tilde{\rho}(\nu_2 - m)}. \qquad (4)$$

The summation is over all integer $m$ and $J_m$ denotes the Bessel function of the first kind. This transformation was derived for the so-called off-resonance case where $\nu_2 - \nu_1 = 1$ and for $\nu_1 \neq n$ and $2\nu_1 \neq n$ where $n$ is an integer. However, as we will demonstrate in the following sections, the threshold for stochasticity we find from this expression is numerically validated even for these exceptional cases. Additionally, the relationship between the canonical variables and the transformed variables is a first-order transformation $I = \tilde{I} + O(\varepsilon_i)$, $\theta = \tilde{\theta} + O(\varepsilon_i)$ [8]. For our purposes, we follow the precedent of Refs. [8–11] in adopting the small perturbation limit such that the transformation of coordinates is of order unity. We therefore drop the tilde coordinates in our subsequent analysis.

## III. WEB STRUCTURE

In order to illustrate the dynamics governed by Eq. (2), we employ the Poincaré cross section (PC), alternatively known as the surface of sections method [14]. We follow the previously established convention for BEW investigations [11] in defining our PC with respect to time. Numerical solutions are plotted in this case by integrating the equations of motion from Eq. (2) for a number of initial conditions, $(\theta,\rho)$ at $\tau = 0$, and sampling these values at a fixed time interval equal to the least common period of the two waves, $\tau_c$.

We show a series of these PC in Fig. 1 for the representative parameters $\nu_1 = 24.2, \nu_2 = 25.2, \kappa_1 = \kappa_2 = 1$, and $\varphi_1 = \varphi_2 = 0$ and increasing values of the perturbation $\varepsilon$, where we have let $\varepsilon_1 = \varepsilon_2$ and defined $\varepsilon = \varepsilon_1$. The initial conditions in each plot are the same; however, the time of integration is larger for smaller wave amplitudes in order to account for the slower orbit frequency around islands in the PC. It is evident from these results that, in the case of small perturbation strength ($\varepsilon = 0.1$), the beat effect produces a web structure in phase space characterized by a series of islands with intervening

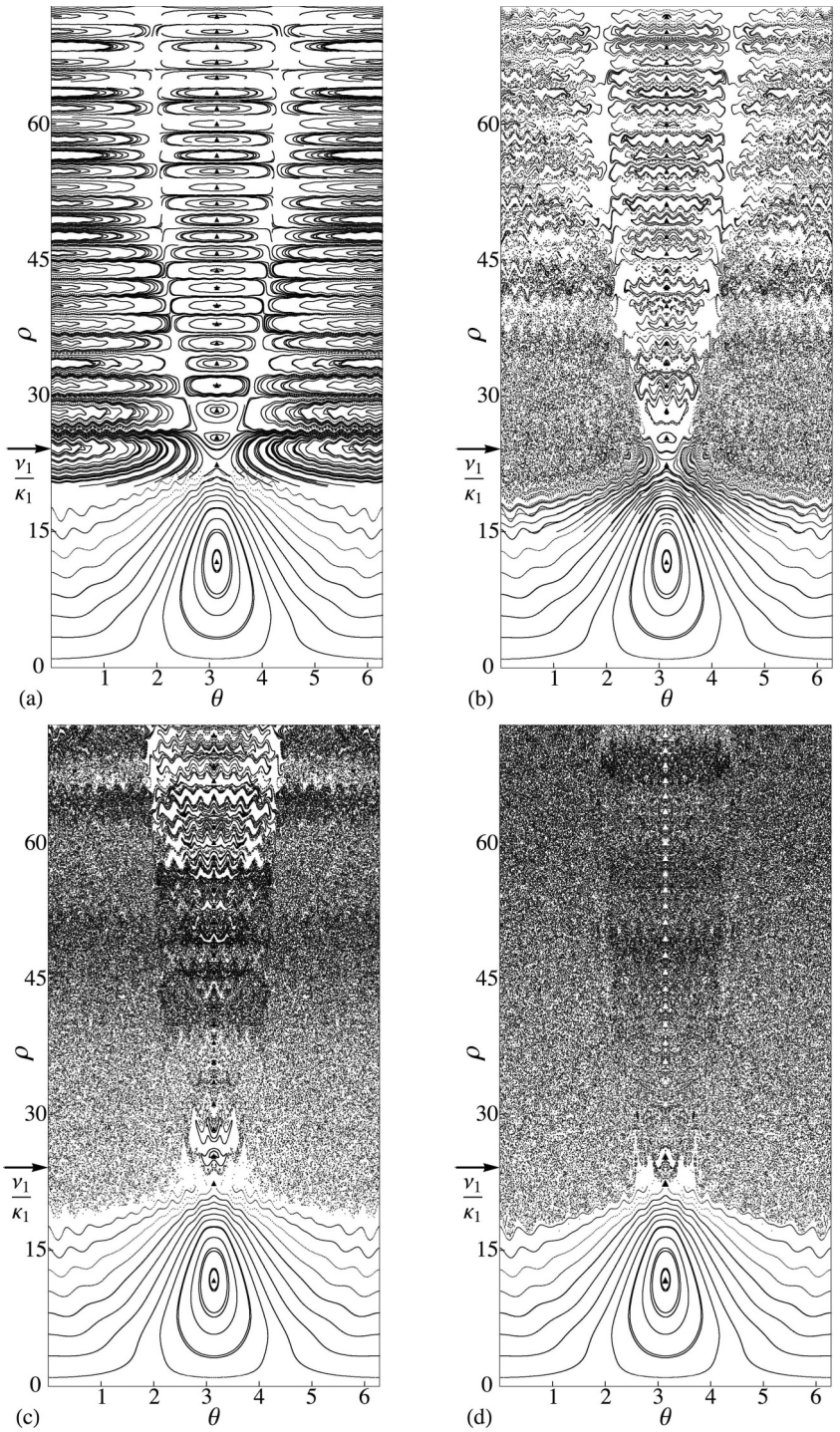


FIG. 1. Poincaré cross sections in time defined at the least common period, $\tau_c$, of the two waves with frequencies $\nu_1, \nu_2$. The same initial conditions are used in all plots with the common wave parameters $\nu_1 = 24.2, \nu_2 = 25.2; \kappa_1 = \kappa_2 = 1; \varphi_1 = \varphi_2 = 0$. The wave amplitudes are also set equal, $\varepsilon_1 = \varepsilon_2 = \varepsilon$, with each plot corresponding to a different amplitude: (a) $\varepsilon = 0.1$, (b) $\varepsilon = 1.1$, (c) $\varepsilon = 2.4$, and (d) $\varepsilon = 3.9$. The markers (▲, △) indicate the locations of the analytically predicted elliptic points.

separatrices around which particle trajectories orbit. This island-populated phase space is well documented [9,11] and can be predicted analytically by using a generating function of the second kind, $F_2 = J[\theta - \tau]$ [15], to canonically transform Eq. (3) to an autonomous form,

$$\hat{H} = \sum_{i=1}^{2} \varepsilon_i^2 S_1^{\nu_i}(\rho) + \varepsilon_1 \varepsilon_2 \cos[\psi + \Delta\varphi] S_6(\rho), \tag{5}$$

where we have used $J = I$, $\psi = \theta - \tau$, $\Delta\varphi = \varphi_2 - \varphi_1$, and we have invoked the beating wave criterion, $\nu_2 - \nu_1 = 1$. In this form, lines of constant $\hat{H}$ describe particle trajectories in the PC, and, therefore, the islands and elliptic points should appear at the fixed points of the autonomous Hamiltonian, i.e., where

$$\dot{\psi} = 0 = \sum_{i=1}^{2} \varepsilon_i^2 \frac{1}{\rho} \frac{\partial S_1^{\nu_i}(\rho)}{\partial \rho} + \varepsilon_1 \varepsilon_2 \cos[\psi + \Delta\varphi] \frac{1}{\rho} \frac{S_6(\rho)}{\partial \rho}$$

$$\dot{I} = 0 = \varepsilon_1 \varepsilon_2 \sin[\psi + \Delta\varphi] S_6(\rho). \tag{6}$$

We denote the location of the analytically predicted elliptic points from this result as markers in Fig. 1 where good agreement is observed with the particle orbits over the plotted phase space. This correspondence helps establish the validity

of the second-order approach in the small-amplitude limit. Furthermore, we note that the web structure predicted from Eqs. (5) and (6) persists with increasing values of $\varepsilon$ for trajectories below the SEW resonant velocity, $\rho = \nu_1/\kappa_1$. This observation permits the continued use of Eq. (6) in characterizing this region of phase for large wave amplitudes, and it is in part because of this expedient result that the coherent acceleration has been the primary focus of previous BEW investigations.

On the other hand, the analysis for trajectories above the SEW resonant conditions $\rho = \nu_1/\kappa_1$ is significantly complicated for wave amplitudes where the second-order description begins to break down. Indeed, as can be seen from Fig. 1, with increasing perturbation strength the predicted web structure gives way to chaotic orbits. The stochasticity first appears with increasing $\varepsilon$ for particles close to the resonant condition and near initial cyclotron phase $\theta \approx 0$ where they are initially in phase with the two waves. Ions with initial cyclotron angle out of phase with the waves $\theta \approx \pi$ remain in trapped orbits until sufficiently large amplitudes are reached ($\varepsilon = 3.9$). For intermediate values of perturbation strength ($\varepsilon = 1.1, 2.4$), the second-order prediction for the elliptic points remains approximately correct near the trapped orbits, and as already noted, below $\kappa_1\rho \approx \nu_1$ the web structure persists for all cases. We also observe that the stochastic region exhibits an upper bound above which the web structure persists and that the lower bound actually extends below the approximation $\kappa_1\rho \approx \nu_1$ for increasing values of $\varepsilon$.

These finite-amplitude effects, which are inherently tied to stochastic acceleration, cannot be predicted by the second-order description in Eq. (5) since the integrability of this expression precludes stochastic dynamics. Spektor and Choueiri [11] circumvented this problem in part for the special case of equal wave amplitudes and wave numbers $\varepsilon_1 = \varepsilon_2, \kappa_1 = \kappa_2$ by identifying—as we have done here through a visual inspection of the PC—the location of the lower bound with the lowest analytical predicted hyperbolic point from Eq. (6). They thus recovered $\rho = \nu_1/\kappa_1$. A similar analysis can be followed from the work of Strozzi *et al.* [10] whose derivation of the autonomous Hamiltonian in the case of obliquely propagating waves allows for a similar (though numerical) calculation of critical points. These estimates for the lower bounds are only approximations, however, in that they do not take into account the root of the stochasticity in phase space. It is for the same reason that these studies do not provide general predictions for the upper bound of the stochastic region or a threshold condition for the onset of stochasticity. The need is thus apparent to give special attention to the chaotic orbits in the system, and in the following section we motivate a description of the dynamics that accounts for these effects.

## IV. STOCHASTIC ONSET

### A. Resonances

One commonly employed method to establish the onset of stochasticity for a dynamical system is the so-called Chirikov condition [16], which states that stochasticity occurs when the separation between resonances in phase space becomes smaller than their average frequency half-widths. The physical reason behind this criterion stems from the frequency mixing produced by the overlap of resonances, which in turn can lead to the decorrelation of particle orbits.

For our dynamical system, we expect to see two classes of resonances: (1) those associated with the SEW resonance [3] between cyclotron motion and the individual wave frequencies such that $\langle\dot{\theta}\rangle/\nu_i = n/m$, where $\langle\rangle$ denotes a time average and $n,m$ are integers, and (2) those associated with the BEW resonance between the cyclotron motion and the beat frequency of the waves $\langle\dot{\theta}\rangle/(\nu_2 - \nu_1) = 1$. Both of these resonances—when they exist—will appear as fixed points in the PC we defined in the previous section. This can be seen explicitly by considering the criterion for the formation of fixed points in this PC,

$$\frac{\nu_c}{\langle\dot{\theta}\rangle} = \frac{p}{s}, \tag{7}$$

where $s, p$ are positive integers; $\nu_c = 1/\tau_c$ is the frequency of the common period of $\nu_1, \nu_2$; $\dot{\theta}$ is the time derivative of the cyclotron phase derived from the nonautonomous Hamiltonian; and $\langle\rangle$ denotes the average over $p$ periods of the sampling time, $\tau_c$. We can see from this prescription that BEW resonance corresponds to first degree islands where $p = 1$, i.e., island chains that only exhibit a single fixed point in the PC. This is exactly the web structure shown in the $\varepsilon = 0.1$ case of Fig. 1 and predicted from the autonomous Hamiltonian in Eq. (5). On the other hand, we anticipate the first islands from interactions with the SEW resonances to occur, where $\langle\dot{\theta}\rangle = \nu_i/\|\nu_i\|$ [4] ($\|..\|$ denotes the nearest integer function). This suggests that these resonances should appear as $p = \|\nu_i\|$ fixed points in the cross section, and, indeed, the effects of these islands can be observed as the periodic ripples in the first degree island orbits.

We have noted from the analytical work in the previous section that the islands due to the BEW effect ($p = 1$) persist for arbitrarily small wave amplitudes. However, as can be seen qualitatively from Fig. 1, the resonances associated with individual waves, $\nu_1, \nu_2$, exist exclusively near the SEW resonant velocities in phase space $\rho = \nu_i/\kappa_i$. It is only with increasing perturbation strength that these higher-degree islands expand into higher velocities, i.e., larger values of $\rho$. This can be explained by considering the source of these respective resonances. In the BEW case, the resonances arise from the difference frequency of the two waves—a fixed parameter—which is inherent to the system. On the other hand, SEW resonances require nonlinear perturbations in the average frequency of cyclotron precession $\langle\dot{\theta}\rangle$ in order to be satisfied. This distinction between resonances is important, for even though the BEW islands exist for small amplitudes, we can see from a qualitative inspection of Fig. 1 that it is the SEW resonances and their overlap with the inherent BEW resonances that lead to stochasticity.

In order to demonstrate this overlap analytically from the Chirikov criterion it is necessary to identify the location of these resonances as well as the perturbation-dependent width. We can analytically do the former through a second-order perturbation analysis. Characterizing the widths, however, in a global and analytical way is significantly more difficult: While there is an established method [16] for determining island widths, the linearity of $H_0 = I$ in our system precludes

the necessary step in this prescription of approximating the motion as a nonlinear pendulum.

In light of this limitation, we are forced to turn in the following section to a numerical analysis to complement our investigation. In a technique inspired by Karney and Bers [3,4], we start by identifying analytically a perturbation-dependent term that predicts the existence of the higher degree SEW resonances and assume that the onset of stochasticity scales with it. We then use this scaling term in conjunction with a numerical investigation of the PC to derive a quasianalytical condition for the onset of stochasticity.

### B. Parameter for stochastic onset

We begin by referring to the nonautononomous, second-order Hamiltonian from Eq. (3) to derive a condition for the formation of SEW islands. As we have noted previously, this integrable Hamiltonian cannot map out stochastic orbits. We therefore only use it to predict the appearance of higher-degree, integrable islands in phase space. The stochastic overlap of these islands is reserved for the numerical discussion.

With this in mind, we first determine the equations of motion from Eq. (3),

$$\dot{\theta} = 1 + \sum_{j=1}^{2} \varepsilon_j^2 \frac{1}{\rho} \frac{\partial S_1^{\nu_j}(\rho)}{\partial \rho} + \varepsilon_1 \varepsilon_2 \cos[\theta - \tau + \Delta\varphi] \frac{1}{\rho} \frac{\partial S_6(\rho)}{\partial \rho}$$

$$\dot{I} = \varepsilon_1 \varepsilon_2 \sin[\theta - \tau + \Delta\varphi] S_6(\rho). \tag{8}$$

From the first line of this expression, we can infer that $\theta \approx \tau + \theta_0 + O(\varepsilon_j^2)$, where $\theta_0$ denotes an initial Larmor angle. For our analysis, we let this initial condition satisfy $\theta_0 + \Delta\varphi = 0$. This is a reasonable assertion as we have already pointed out from the plots in Fig. 1 that this relative phase with respect to the BEW waves is the most favorable for the onset of stochasticity. For small potential amplitudes, we consequently see that $\langle \dot{I} \rangle \sim O(\varepsilon_j^4)$, which allows us to assume constancy to second order for the action in our estimates. We further use the approximation $\theta \approx \tau + \theta_0 + O(\varepsilon_j^2)$ to assert the periodic term in $\dot{\theta}$ is constant when taking the average indicated in Eq. (7). This yields

$$\langle \dot{\theta} \rangle \approx 1 + \sum_{j=1}^{2} \varepsilon_j^2 \frac{1}{\rho} \frac{\partial S_1^{\nu_j}(\rho)}{\partial \rho} + \varepsilon_1 \varepsilon_2 \frac{1}{\rho} \frac{\partial S_6(\rho)}{\partial \rho}. \tag{9}$$

With this expression, we first consider the resonances produced by the lower-frequency wave such that $\langle \dot{\theta} \rangle / \nu_1 = n/m$, where $n$ and $m$ are integers. For different values of $n,m$, we follow a treatment similar to that of Karney in defining a parameter $R = \|\nu_1\| \langle \dot{\theta} \rangle - \nu_1$ such that, from Eq. (9),

$$R = -\delta + \|\nu_1\| \left[ \sum_{i=1}^{2} \varepsilon_i^2 \frac{1}{\rho} \frac{\partial S_1^{\nu_i}(\rho)}{\partial \rho} + \varepsilon_1 \varepsilon_2 \frac{1}{\rho} \frac{\partial S_6(\rho)}{\partial \rho} \right], \tag{10}$$

where $\delta = \nu_1 - \|\nu_1\|$. Large values of $|R|$ correspond to the onset of additional resonances and islands in the BEW PC. Indeed, $R = 0$ corresponds to the first onset of islands where $n = 1, m = \|\nu_1\|$, while deviations from $R = 0$ indicate the formation of increasingly nonlinear $\langle \dot{\theta} \rangle \neq 1$ resonances. This suggests an appropriate scaling term for the onset of stochasticity,

$$F_1 = f(\delta) \|\nu_1\| \left[ \sum_{i=1}^{2} \varepsilon_i^2 \frac{1}{\rho} \frac{\partial S_1^{\nu_i}(\rho)}{\partial \rho} + \varepsilon_1 \varepsilon_2 \frac{1}{\rho} \frac{\partial S_6(\rho)}{\partial \rho} \right], \tag{11}$$

where we have incorporated the dependence on $\delta$ into a function $f(\delta)$. We find a similar result for the onset of islands around the resonances of the second wave,

$$F_2 = f(\delta) \|\nu_2\| \left[ \sum_{i=1}^{2} \varepsilon_i^2 \frac{1}{\rho} \frac{\partial S_1^{\nu_i}(\rho)}{\partial \rho} + \varepsilon_1 \varepsilon_2 \frac{1}{\rho} \frac{\partial S_6(\rho)}{\partial \rho} \right]. \tag{12}$$

In the case of large $\nu_1 \gg 1$, these results converge to a global parameter for island overlap at the resonances of each wave. For the remainder of the discussion then, we invoke this condition in Eq. (11) by defining $F = F_1 \to F_2$ and similarly $\|\nu_i\| \to \nu_i$. We note here that solving this term for the case where $F = 0$ corresponds to calculating the location of the elliptic points in the $\nu_c$ cross section from Eq. (5). This is not surprising since following the same treatment above for the BEW resonance (substituting $\nu_1 \to 1; n = m = 1$) should produce a condition for the formation of $p = 1$ islands in the PC.

For higher-order resonances and $F \neq 0$, however, we seek a simpler form of Eq. (11). In the limit of large $\kappa_i \rho > \nu_i + (\frac{1}{2}\nu_i)^{1/3}$, we see that this term can be expressed as (Appendix A),

$$F = f(\delta) \frac{\nu_1^2 \pi}{\sin(\pi\delta)} \Big\{ [\varepsilon_1 A_1(\rho) \sin\alpha_1 + A_2(\rho)\varepsilon_2 \sin\alpha_2]^2 - [\varepsilon_1 A_1(\rho) \cos\alpha_1]^2 - [\varepsilon_2 A_2(\rho) \cos\alpha_2]^2 - \varepsilon_1 \varepsilon_2 \frac{[A_1^4(\rho) + A_2^4(\rho)]}{A_1(\rho) A_2(\rho)} \cos\alpha_1 \cos\alpha_2 \Big\}, \tag{13}$$

where we have defined

$$A_i(\rho) = \frac{\left| H_{\nu_i}^{1'}(\kappa_i \rho) \right|}{\rho}$$

$$\alpha_i = \left\{ \left[ (\kappa_i \rho)^2 - \nu_i^2 \right]^{1/2} - \nu_i \cos^{-1}\left( \frac{\nu_i}{\kappa_i \rho} \right) - \frac{\pi}{4}(1 - 2\delta) \right\}, \tag{14}$$

where $H_{\nu_i}^1$ denotes the Hankel function of the first kind and the derivative is with respect to $\rho$. In order to simplify this result further, it is desirable to find a method for factoring the additional terms. With this purpose in mind, we show in Appendix A that in the large-velocity limit ($\kappa_2\rho, \kappa_1\rho \gg \nu_2, \nu_1$) and assuming $\kappa_2 \sim \kappa_1$, we can reduce the second term to

$$\frac{\nu_1^2 \pi}{\sin(\pi\delta)} [\varepsilon_1 A_1(\rho) \cos\alpha_1 + A_2(\rho)\varepsilon_2 \cos\alpha_2]^2, \tag{15}$$

such that the total expression for the scaling parameter is given by

$$F = f(\delta) \frac{\nu_1^2 \pi}{\sin(\pi\delta)} \{ [\varepsilon_1 A_1(\rho) \sin\alpha_1 + \varepsilon_2 A_2(\rho) \sin\alpha_2]^2 - [\varepsilon_1 A_1(\rho) \cos\alpha_1 + \varepsilon_2 A_2(\rho) \cos\alpha_2]^2 \}. \tag{16}$$

Finally, we note that since both $\alpha_1$ and $\alpha_2$ are rapidly varying functions of $\rho$, we need retain only the amplitudes of the

scaling terms. This suggests that the correct parameter for the onset of stochasticity is given by

$$F = f(\delta)G(\nu_1,\varepsilon_1,\varepsilon_2,\kappa_1,\kappa_2,\rho), \tag{17}$$

where we have folded the constants into the function $f(\delta)$ and defined

$$G(\nu_1,\varepsilon_1,\varepsilon_2,\kappa_1,\kappa_2,\rho) = \nu_1[\varepsilon_1 A_1(\rho) + \varepsilon_2 A_2(\rho)]. \tag{18}$$

This final expression provides a simple term for the onset of stochasticity in the case of perpendicularly propagating BEW that is valid for ion velocities greater than the wave velocity and for normalized wave numbers that satisfy $\kappa_2 \sim \kappa_1$. It is of particular importance that we were able to factor this result since this form suggests that the BEW effect has a lower threshold for stochasticity than the case with two nonbeating waves. We postpone this discussion for the moment, however, in order to numerically verify Eq. (17) and determine the appropriate form of $f(\delta)$. To this end, in the following section we use a numerically calculated criterion—the maximum Lyapunov exponent—for stochasticity in phase space.

## V. NUMERICAL ANALYSIS

For dynamical systems, the maximum Lyapunov exponent $\lambda$ provides a measure of the separation $|\mathbf{Z}|$ in phase space of two particle trajectories as it depends on the small initial separation, $|\mathbf{Z_0}|$ [14],

$$|\mathbf{Z}| = |\mathbf{Z_0}|e^{\lambda\tau}. \tag{19}$$

Since a positive $\lambda$ corresponds to exponentially diverging trajectories, this parameter can serve as a metric for the degree of stochasticity in a local region of phase space. For our system, we used a prescribed algorithm [17] to numerically estimate the maximum Lyapunov exponents (MLE) of Eq. (2) as a function of initial conditions, $(\theta,\rho)$ at $\tau = 0$. This method yielded values of $\lambda$ that converged for $\tau < 150$ in all cases considered. Additionally, in order to approximate this stochastic parameter as a function strictly of $\rho$, we selected five equally spaced values of $\theta$ in the PC for a fixed $\rho$ and averaged them to find $\overline{\lambda}(\rho) = \frac{1}{5}\sum_{n=1}^{5}\lambda(n2\pi/5,\rho)$.

We show $\overline{\lambda}(\rho)$ in Fig. 2 for the same wave parameters as the four cases in Fig. 1. Based on the criterion that $\overline{\lambda} > 0$ corresponds to the appearance of nonintegrable, diverging orbits, we see that the average MLE accurately predicts the trends depicted in the BEW PCs. For the nonstochastic case in Fig. 1 ($\varepsilon = 0.1$), the value of the average MLE is $\overline{\lambda} \approx 0$ for the entire range of phase space. On the other hand, the MLE becomes finite with increasing perturbation strength. This occurs first in the vicinity of the SEW resonant condition $\rho = \nu_1/\kappa_1$, which as can be seen from the $\varepsilon = 1.1$ case of Fig. 1 is where stochasticity first appears in the PC. As the normalized amplitude becomes even larger, the region of stochasticity extends to a wider range of velocities around the resonant SEW velocity. This trend reflects the orbits shown in the corresponding PC where stochasticity is most prevalent near the SEW resonant condition but gives way to the BEW web structure away from this velocity. A more detailed visual inspection of these PCs reveals that while nonzero, finite values of the MLE indicate the first appearance of stochastic orbits, the phase space becomes dominated by chaotic orbits above a

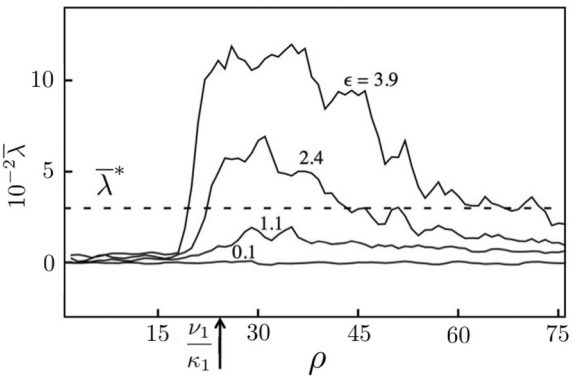


FIG. 2. The angle-averaged maximum Lyapunov exponent as a function of normalized velocity for the same wave parameters as in Fig. 1. The dashed line represents the stochastic value of MLE where the majority of orbits in phase space of the corresponding PC are chaotic.

finite threshold value that we denote $\overline{\lambda}^\star \approx 3 \times 10^{-2}$. We adopt this numerical estimate as a local metric for stochasticity in the following discussion.

Armed with this criterion for stochasticity, we now can investigate the validity of the analytically derived term in Eq. (17) by examining the dependence of the average MLE on the stochasticity parameter. In particular, since larger values of $F$ correspond to increased stochasticity, we anticipate a monotonic relationship between $F$ and $\overline{\lambda}$ where at a threshold value, $F^*$, stochasticity will occur, i.e., $\overline{\lambda}(F^*) = \overline{\lambda}^*$. The term $f(\delta)$, however, is an unknown function, which bars us from explicitly examining the impact of the stochastic parameter, $F$. To overcome this limitation, we make the *a priori* assumption that $f(\delta)$ is approximately constant for our analysis, and we instead plot $\overline{\lambda}$ as a function of the defined term $G(\nu_1,\varepsilon_1,\varepsilon_2,\kappa_1,\kappa_2,\rho)$ in Fig. 3.

We made our numerical investigation of this term comprehensive by generating values of $G$ from a wide range of possible parameters. This was accomplished by randomly selecting 1000 sets of values $(\varepsilon_1,\varepsilon_2,\nu_1,\kappa_1,\kappa_2,\rho)$ that satisfied $G < 0.4$ from the parameter spaced defined by $\varepsilon_1 \in (1,20)$, $\varepsilon_2 \in (1,20)$, $\nu_1 \in (10,100)$, $\kappa_2 \in (0.7,1.2)$, and $\rho \in (1,100)$.

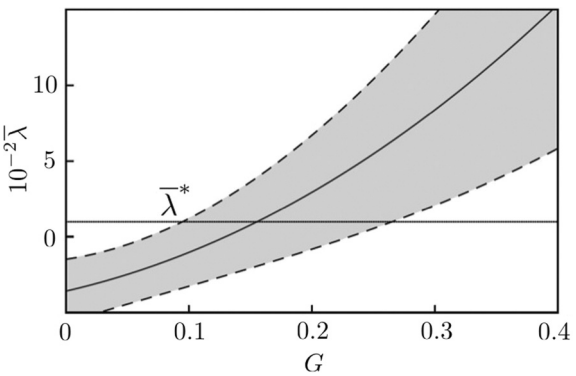


FIG. 3. The average MLE plotted as a function of the stochastic parameter, $G$. The solid line indicates the mean trend while the gray region marks the 93% confidence interval for the numerically calculated values. The stochastic condition $\overline{\lambda}^*$ is shown as a horizontal line.

On-resonance values $\nu_1 = n$, where $n$ is an integer were included in this range, but since $\kappa_1 = 1$ by virtue of our normalization scheme, it was not necessary to vary this parameter. Using these 1000 values, we then determined numerically the corresponding phase-averaged MLE, $\bar{\lambda}$. The mean trend from this calculation for $G(\lambda)$ is shown in Fig. 3 along with confidence intervals, denoted by the shaded range, where 93% of the 1000 selected points fell.

In spite of the wide range of initial conditions, we see the anticipated monotonically increasing trend of $\bar{\lambda}$ with $G$. This dependence serves to validate our derivation of $G$ as a correct scaling parameter for the local stochastic state of phase space—even when $\nu_1 = \|\nu_1\|$ where our analytical derivation is not strictly valid. Moreover, we can use our threshold value $\bar{\lambda}^* = 3 \times 10^{-2}$ to estimate from Eq. (17) that phase space becomes stochastic when $G > 0.1$–$0.27$. Our assumption that $f(\delta)$ is approximately constant is thus borne out with an appropriate range of values given by $f(\delta) = 3.7$–$10$. It is important to note that this spread in value persists even when the above investigation is repeated only allowing for a constant off-resonance condition that satisfies $\delta \neq 0$. This suggests that the uncertainty in $f(\delta)$ is not a result of the breakdown in the validity of Eq. (17) in the on-resonance case. Rather, this variance likely stems from small differences in the dynamical orbits brought about by the widely different wave parameters we considered.

We note here that for the SEW case ($\varepsilon_2 \to 0$) Karney [4] numerically found $f(\delta) = 4$ while Fukuyama [18] with a less stringent condition of stochasticity found $f(\delta) = 6.7$. Both of these analyses were limited in scope, however, in that the numerical analyses were performed for one value of $\|\nu_1\|$ and a small range of $\rho$ values. An analysis over a wider range of parameters introduces less certainty for the estimate of $f(\delta)$. We can confirm this explicitly by investigating our BEW result, $F = f(\delta)G$, in the SEW limit ($\varepsilon_2 = 0$) where our expression converges to the parameters derived in these previously cited studies. With this term, we have repeated the above analysis for SEW over the same range of wave variables to find $f(\delta) = 5$–$10$. This range lies just above the value reported by Karney—a difference that likely stems from the definition for when phase space is primarily stochastic. The more important insight from this result, however, is that the precision of the previously reported SEW case is an artifact of the small range of values that were numerically investigated.

With this in mind, our above analysis allows to assert the final, linear result for the stochastic parameter in the BEW case,

$$\alpha < \nu_1(\varepsilon_1 A_1 + \varepsilon_2 A_2), \tag{20}$$

where $\alpha = 0.1$–$0.27$. This simplified form incorporates the effects of both waves while it reduces to the previously derived SEW stochasticity limit for small $\varepsilon_2 \to 0$. This expression also provides a means for characterizing the upper bound of stochasticity in the BEW system for a fixed set of wave parameters. Indeed, for finite $\varepsilon_1$,$\varepsilon_2$, we see the upper bound in stochastic space occurs where $\rho$ is sufficiently large that Eq. (20) is violated. This is shown in Fig. 4 where we have plotted the analytical result for $\varepsilon = \varepsilon_1 = \varepsilon_2$ along with the numerically calculated upper bound ($\alpha = 0.27$ was used in this case).

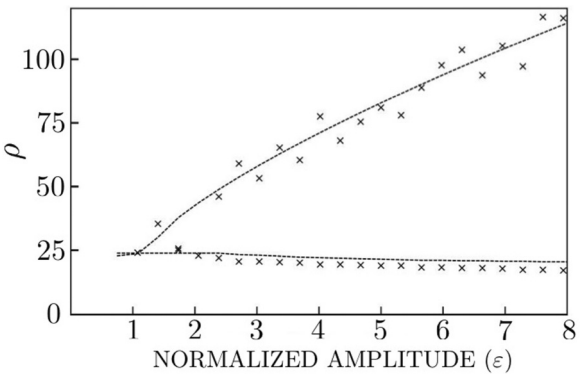


FIG. 4. Upper and lower bounds of stochastic region as a function of normalized wave amplitude. The markers represent numerically calculated values for the same wave parameters as Fig. 1 with $\varepsilon = \varepsilon_1 = \varepsilon_2$. The dashed lines are the analytically derived bounds.

A similar calculation for the lower bound in phase space is precluded by the underlying assumptions we made in deriving $A_1(\rho)$, $A_2(\rho)$ in Eq. (14). Specifically, the Hankel functions are approximations for the amplitude of the Bessel function that are valid only in the limit $\rho\kappa_i > \nu_i + (\frac{1}{2}\nu_i)^{1/3}$, and while these functions diverge at $\rho \to 0$, we anticipate from our numerical observations of phase space that the coefficients $A_1(\rho)$, $A_2(\rho)$ should in fact approach 0. We therefore are forced to search for an approximate form of the coefficients in the small-$\rho$ limit. A reasonable choice is to infer that $A_i(\rho)$ will continue to scale with the amplitude $J'(\kappa_i\rho)$. This is expedient since it not only approaches 0 for small $\rho$ but monotonically increases in the prescribed range until exhibiting a local maximum near $\rho \approx \nu_i/\kappa_i$. Given these considerations, then, we can recover an approximate form for these coefficients by extending the definition of $A_1$, $A_2$ to encompass the lower values of $\rho$,

$$A_i(\rho) = \frac{1}{\rho}[\mathrm{envl}(\rho)], \tag{21}$$

where in order to ensure continuity we have defined envl as a fourth degree interpolating polynomial that satisfies

$$\mathrm{envl}(\rho) = \begin{cases} \left|H^{1'}_{\nu_i}(\kappa_i\rho)\right| & \text{for } \kappa_i\rho \geqslant \nu_i + \left(\frac{1}{2}\nu_i\right)^{1/3} \\ J'_{\nu_i}(\kappa_i\rho) & \text{for } \kappa_i\rho < \nu_i. \end{cases}$$

From this result, we plot the predicted lower bound of the stochastic region as a function of $\varepsilon$ in Fig. 4 along with the numerically observed values. We see general agreement in spite of the approximations we made in deriving this term. In particular, the lower bound is characterized by the phase velocity of the slower wave $\rho = \nu_i/\kappa_i$ with a weak dependence on the perturbation strength—a similar result to that previously reported for SEW [4] and a special case of BEW [11].

The modified definitions of $A_1(\rho)$ and $A_2(\rho)$ allow us to determine the full extent of phase space that is stochastic, and in some special cases, they can be used in conjunction with Eq. (20) to identify analytically the minimum set of wave amplitudes $\varepsilon_1$,$\varepsilon_2$ for when stochasticity first appears. Specifically, when $\nu_1 \gg 1$ and $\nu_1/\kappa_1 \approx \nu_2/\kappa_2$, such as may be found in acoustic modes, we see that both coefficients exhibit

maxima at $\rho \approx \nu_1/\kappa_1$. At this maximum value and in the limit of large normalized frequency, the Bessel functions can be simplified to $J_x'(x) \approx x^{-2/3}$ [19] and the coefficients become $A_i(\rho) = \kappa_i^2 \nu_i^{-5/3}$. We substitute this into the above criterion to find the threshold condition for the onset of stochasticity,

$$\alpha = \kappa_1^2 \nu_1^{-1}\left(\varepsilon_1 \nu_1^{1/3} + \varepsilon_2 \nu_2^{1/3}\right). \tag{22}$$

This concise form, which is applicable to perpendicularly propagating acoustic modes, shows explicitly that the relationship between perturbation strength for onset is linear and the strength of each mode is weighted by the frequency. Of course, the validity of this expression is violated for waves with greater dispersion, but even in this limit, it still can serve as a first test for stochasticity. More generally, this linear dependence is an important consideration for the next section where we demonstrate how stochasticity can be achieved with BEW for lower input energy densities of the exciting waves than with the SEW and non-BEW two-wave systems.

## VI. COMPARISON AMONG SEW, BEW, AND NONBEATING WAVES

By comparing the SEW limiting case of Eq. (20) to the full expression, we see that stochasticity can be achieved with BEW for lower individual wave-amplitude values. A more important question when comparing the efficiency of the two processes, however, is whether stochastic onset occurs for a lower total energy density in the BEW case. To consider this possibility, we first note that the total energy density of each electrostatic wave depends quadratically on the potential [20] such that

$$W = (\beta_1 \varepsilon_1)^2 + (\beta_2 \varepsilon_2)^2, \tag{23}$$

where $W$ denotes the total energy density and $\beta_1, \beta_2$ are two constants that depend on the individual wave parameter, $\nu_i, \kappa_i$. Let us denote $\eta = (\beta_1 \varepsilon_1)^2 / W$, i.e., the fractional energy density in the first mode. The threshold for stochasticity with BEW then becomes

$$\nu_1 \sqrt{W_{\mathrm{BEW}}}[A_1(\rho)\beta_1^{-1}\sqrt{\eta} + A_2(\rho)\beta_2^{-1}\sqrt{1-\eta}] = \alpha. \tag{24}$$

Similarly, the thresholds for the individual SEW are

$$\nu_1 \sqrt{W_{1(\mathrm{SEW})}}\beta_1^{-1} A_1(\rho) = \alpha, \quad \nu_2 \sqrt{W_{2(\mathrm{SEW})}}\beta_2^{-1} A_2(\rho) = \alpha, \tag{25}$$

where we have assumed the total energy density is concentrated in each mode. The ratio of the required energy density for the onset of stochasticity of BEW compared to that required for the onset of stochasticity for each SEW is thus given by

$$\left(\frac{W_{1(\mathrm{SEW})}}{W_{\mathrm{BEW}}}\right)^{1/2} = [\sqrt{\eta} + \gamma\sqrt{1-\eta}],$$
$$\left(\frac{W_{2(\mathrm{SEW})}}{W_{\mathrm{BEW}}}\right)^{1/2} = [\gamma^{-1}\sqrt{\eta} + \sqrt{1-\eta}], \tag{26}$$

where we have denoted $\gamma = \frac{A_2\beta_1}{A_1\beta_2}$ and made the simplifying assumption that $\nu_2/\nu_1 \approx 1$. The BEW process has a lower energy density threshold for the onset stochasticity if there exists $\eta \in (0,1)$ when both expressions are greater than 1. It is evident from Eq. (26) that this condition is satisfied provided $\gamma \neq 0, \infty$. These limiting cases can be discounted, however, as they represent the nonphysical scenarios where the energy content of the one of the BEW is 0.

BEW—subject to the assumptions outlined above—thus will produce stochasticity for lower energy densities than a SEW. This is a significant result as the onset of stochasticity has been shown to coincide with a threshold for plasma heating [21,22]. The onset of heating therefore may occur for lower levels of energy density with BEW, though of course once this threshold has been exceeded, the level of heating is dependent on the self-consistent exchange of energy of both the SEW and BEW processes. An analysis of this is outside the scope of this paper.

For a final comparison, we examine the case for when there are two waves that *do not* satisfy the beating criterion, i.e., there is no beat resonance. The second-order cross term in Eq. (3) that is proportional to $\varepsilon_1\varepsilon_2$ consequently disappears in the derivation outlined in Sec. IV B and the threshold for the onset of stochasticity becomes

$$\alpha = \{[\varepsilon_1 A_1(\rho)]^2 + [\varepsilon_2 A_2(\rho)]^2\}^{1/2}, \tag{27}$$

where we have assumed the same constant for $f(\delta)$. Comparing this result with the BEW case, we immediately see that without the benefit of the beat effect, the onset condition for stochasticity is higher for a given energy density. This stems mathematically from the missing cross-term in the threshold and physically from the loss of the additional resonances in phase space.

Moreover, without the beat effect, the two waves do not appear to offer any energy-saving advantage over SEW stochasticity. We can see this explicitly by expressing Eq. (27) in terms of energy densities,

$$\nu_1 \sqrt{W_{n\mathrm{BEW}}}\left[A_1^2(\rho)\beta_1^{-2}\eta + A_2^2(\rho)\beta_2^{-2}(1-\eta)\right]^{1/2} = \alpha, \tag{28}$$

where we have denoted the total energy density between the nonbeating waves as $W_{n\mathrm{BEW}}$. When we compare the cases for the energy density for the onset of stochasticity with the SEW case, we find

$$\frac{W_{1(\mathrm{SEW})}}{W_{n\mathrm{BEW}}} = \eta + \gamma^2(1-\eta), \quad \frac{W_{2(\mathrm{SEW})}}{W_{n\mathrm{BEW}}} = \gamma^{-2}\eta + (1-\eta). \tag{29}$$

Again, the conditions for when the non-BEW process is superior to the SEW occurs when $W_{1(\mathrm{SEW})}/W_{n\mathrm{BEW}}$, $W_{2(\mathrm{SEW})}/W_{n\mathrm{BEW}} > 1$. Solving from the above equations, we see this condition cannot be satisfied for $\eta \in (0,1)$. Therefore, we must conclude that, in the non-BEW case, even though lower individual wave amplitudes can lead to the onset of stochasticity, this process is not superior to the SEW case when examined in the context of total wave energy density.

## VII. OBLIQUE PROPAGATION

The above findings have applications for physically realizable cases where collinear, perpendicularly-propagating

modes are employed. However, in order to extend this discussion to encompass situations where oblique propagation is allowed, we consider briefly in this section the impact of a finite parallel wave number.

When including the effects of parallel wave propagation, the Hamiltonian from Eq. (2) becomes

$$H = I + \frac{1}{2}V_z^2 + \sum_{i=1}^{2} \varepsilon_i \cos(\kappa_i \rho \sin\theta + \kappa_{iz} Z - \nu_i \tau + \varphi_i), \tag{30}$$

where $\kappa_{iz}$ denotes the normalized wave number in the parallel direction and $V_z$ is the normalized velocity in the parallel direction. It is evident from this form that the investigation of stochasticity is complicated by the necessity of examining a large range of cyclotron resonances at $m + \kappa_{iz} V_z - \nu_i = 0$, where $m$ is an integer. We can avoid this difficulty, however, by exploiting the fact that in many physically realizable experiments, the parallel wave number of the electrostatic modes coupled into the plasma is dictated by the geometry of the antenna that launches the waves. This allows us to make the approximation that regardless of frequency, the parallel wave number is constant, i.e., $\kappa_{1z} = \kappa_{2z}$.

In this special case of equal wave numbers, Strozzi *et al.* [10] demonstrated from a second-order perturbation analysis that to second order $V_z$ is a constant of motion. As a consequence, we can infer that $Z = V_z \tau$ where initial conditions are incorporated into the phases $\varphi_i$. This observation permits us to convert Eq. (2) into the more general form of Eq. (30) through the following substitutions:

$$H \to H - \tfrac{1}{2}V_Z^2 \quad \nu_i \to \nu_i - \kappa_z V_z. \tag{31}$$

We can apply this same transformation to Eq. (20) to yield the limit for the onset of stochasticity in the case where the wave numbers in the parallel direction are equal,

$$\alpha < \nu_1 [\varepsilon_1 \tilde{A}_1(\rho) + \varepsilon_2 \tilde{A}_2(\rho)], \tag{32}$$

where we have defined $\tilde{A}_i = A_i(\nu_i \to \nu_i - \kappa_z V_z)$. This criterion reduces to the previously derived result [4] in the SEW limit ($\varepsilon_2 \to 0$). Moreover, this expression illustrates that the effect of the parallel component is to lower the threshold in phase space of the stochastic layer by $\kappa_z V_z$.

## VIII. FINAL DISCUSSION

The above results offer a number of new insights into the BEW process. For example, while it has been pointed out in previous work [9] that BEW can lead to ion acceleration without stochasticity, only particles subject to the appropriate initial conditions will experience significant acceleration along the separatrices of the web structure. The rest remain trapped in coherent orbits around the first degree BEW islands. It is only when a region of the web becomes stochastic that the coherently accelerated ions can reach even higher energies by their random walk through chaotic phase space. Our new understanding of when and how this stochastic onset occurs therefore allows for improved estimates of single-particle energization through BEW.

The onset of stochasticity has additional bearing on the heating of a plasma with BEW. In particular, our condition for the onset of stochasticity suggests that there is an approximate threshold in amplitude for the heating of a plasma with the BEW, and the linear dependence of this threshold on wave amplitude indicates that BEW stochasticity can occur for lower energy densities than with SEW or two nonbeating waves. For experiments limited in energy density, it therefore seems preferable to use two beating modes to achieve heating. This result complements our previous numerical and analytical work [13] where we showed through a non-self-consistent model of ion dynamics that, above the stochastic threshold, BEW produces greater heating than SEW heating.

As a final consideration, the existence of a stochastic threshold and the subsequent decorrelation in particles orbits also allows (through a Markovian assumption) for part of the BEW wave interaction to be modeled as a diffusive process. This can lead to a simplified and self-consistent model for the interaction of the waves with a plasma.

## IX. CONCLUSION

Through a combination of perturbation theory and numerical analysis, we have arrived at an expression for the onset and bounds in phase space of stochasticity for the case of two beating electrostatic waves. We have verified our expression numerically even in the case of on-resonance $\nu_1 = \|\nu_1\|$, which was not explicitly accounted for in our analytical derivation, and we have found that our result reduces in the single wave case to the SEW threshold previously derived by Karney and Fukuyama. Furthermore, we have showed that even though we derived the stochastic condition under the assumption of perpendicularly propagating waves, the effects of parallel wave numbers can be incorporated through a simple canonical substitution.

The physical implications of this work can be seen from the linear dependence of the stochastic condition on the amplitudes of the two BEW. In particular, we have showed how this dependence translates to a lower required energy density for the onset of stochasticity than the case with a SEW or two, noninteracting waves. Since the onset of stochasticity is correlated with the onset of ion heating, this result supports the conclusion that the BEW mechanism is an energetically efficient process with applications in both single-particle acceleration and plasma heating.

## APPENDIX A: SIMPLIFICATION OF $F$

For these considerations, we employ the asymptotic approximation for the Bessel function in the $x \gg m + (\frac{1}{2}m)^{1/3}$ [19] limit,

$$J_m(x) = \left(\frac{2}{\pi}\right)^{1/2} \frac{\cos\left[(x^2 - m^2)^{1/2} - m\cos^{-1}\left(\frac{m}{x}\right) - \frac{\pi}{4}\right]}{(x^2 - m^2)^{1/4}}. \tag{A1}$$

With this expression, we see that the cross-term in $F$ becomes to leading order

$$\frac{1}{\rho}\frac{\partial S_6(\rho)}{\partial \rho} = \frac{1}{2\pi\rho^4}\left[S_6^A(\rho) + S_6^B(\rho)\right], \tag{A2}$$

where we have defined

$$S_6^A(\rho) = -\sum_m \left[\frac{(\kappa_2\rho)^2-(m+1)^2}{(\kappa_1\rho)^2-m^2}\right]^{1/4} \frac{m}{\nu_1-m}(\{[(\kappa_2\rho)^2-(m+1)^2]^{1/2}+[(\kappa_1\rho)^2-(m)^2]^{1/2}\}\cos C_1 + \{[(\kappa_2\rho)^2-(m+1)^2]^{1/2}-[(\kappa_1\rho)^2-(m)^2]^{1/2}\}\cos C_2) \tag{A3}$$

$$S_6^B(\rho) = -\sum_m \left[\frac{(\kappa_1\rho)^2-(m-1)^2}{(\kappa_2\rho)^2-m^2}\right]^{1/4} \frac{m}{\nu_2-m}(\{[(\kappa_1\rho)^2-(m-1)^2]^{1/2}+[(\kappa_2\rho)^2-(m)^2]^{1/2}\}\cos D_1 + \{[(\kappa_1\rho)^2-(m-1)^2]^{1/2}-[(\kappa_2\rho)^2-(m)^2]^{1/2}\}\cos D_2) \tag{A4}$$

and condensed the arguments of the cosine functions to

$$\begin{aligned} C_1 &= [(\kappa_2\rho)^2-(m+1)^2]^{1/2}+[(\kappa_1\rho)^2-(m)^2]^{1/2}-m\cos^{-1}\left(\frac{m}{\kappa_1\rho}\right)-(m+1)\cos^{-1}\left(\frac{m+1}{\kappa_2\rho}\right)-\frac{\pi}{2} \\ C_2 &= [(\kappa_1\rho)^2-(m)^2]^{1/2}-[(\kappa_2\rho)^2-(m+1)^2]^{1/2}-m\cos^{-1}\left(\frac{m}{\kappa_1\rho}\right)+(m+1)\cos^{-1}\left(\frac{m+1}{\kappa_2\rho}\right) \end{aligned} \tag{A5}$$

$$\begin{aligned} D_1 &= [(\kappa_2\rho)^2-(m-1)^2]^{1/2}+[(\kappa_1\rho)^2-(m)^2]^{1/2}-(m-1)\cos^{-1}\left(\frac{m-1}{\kappa_1\rho}\right)-m\cos^{-1}\left(\frac{m}{\kappa_2\rho}\right)-\frac{\pi}{2} \\ D_2 &= [(\kappa_1\rho)^2-(m-1)^2]^{1/2}-[(\kappa_2\rho)^2-(m)^2]^{1/2}-(m-1)\cos^{-1}\left(\frac{m-1}{\kappa_1\rho}\right)+m\cos^{-1}\left(\frac{m}{\kappa_2\rho}\right). \end{aligned} \tag{A6}$$

In order to evaluate the expressions in (A3) and (A4), we follow Ref. [4] in expanding the coefficients of the rapidly varying, sinusoidal terms about $m=\nu_1$ in $S_6^A$ and $m=\nu_2$ in $S_6^B$,

$$\begin{aligned} S_6^A &= -\nu_1\frac{\Gamma_2}{\Gamma_1}\left[\left(\Gamma_2^2+\Gamma_1^2\right)\sum_m\frac{\cos C_1}{\nu_1-m}+\left(\Gamma_2^2-\Gamma_1^2\right)\sum_m\frac{\cos C_2}{\nu_1-m}\right], \\ S_6^B &= -\nu_2\frac{\Gamma_1}{\Gamma_2}\left[\left(\Gamma_2^2+\Gamma_1^2\right)\sum_m\frac{\cos D_1}{\nu_2-m}+\left(\Gamma_1^2-\Gamma_2^2\right)\sum_m\frac{\cos D_2}{\nu_2-m}\right], \end{aligned} \tag{A7}$$

where we have defined

$$\Gamma_i^2 = \left[(\kappa_i\rho)^2-\nu_i^2\right]^{1/2}. \tag{A8}$$

We similarly expand the arguments of the cosine functions. For example,

$$\sum_m\frac{\cos C_1}{\nu_1-m} = \mathrm{Re}\left\{\exp\left[i\left(\Gamma_1^2+\Gamma_2^2-\nu_1 b_1-\nu_2 b_2-\frac{\pi}{2}\right)\right]\sum_m\frac{\exp[i(b_1+b_2)(\nu_1-m)]}{\nu_1-m}\right\}, \tag{A9}$$

where we have defined $b_1=\cos^{-1}(\frac{\nu_1}{\kappa_1\rho})$ and $b_2=\cos^{-1}(\frac{\nu_2}{\kappa_2\rho})$. We can evaluate this summation for the case of $\kappa_1\rho \gg \nu_1$ [4,19],

$$\sum_m\frac{\cos C_1}{\nu_1-m} = \pi\frac{\sin\left[\Gamma_1^2+\Gamma_2^2-\nu_1 b_1-\nu_2 b_2+\pi\delta\right]}{\sin(\pi\delta)}. \tag{A10}$$

We follow a similar treatment for the additional terms in (A7),

$$\begin{aligned} \sum_m\frac{\cos C_2}{\nu_1-m} &= \pi\frac{\cos\left[\Gamma_1^2-\Gamma_2^2-\nu_1 b_1+\nu_2 b_2+\pi\delta\right]}{\sin(\pi\delta)}, \\ \sum_m\frac{\cos D_1}{\nu_2-m} &= \pi\frac{\sin\left[\Gamma_1^2+\Gamma_2^2-\nu_1 b_1-\nu_2 b_2+\pi\delta\right]}{\sin(\pi\delta)}, \\ \sum_m\frac{\cos D_2}{\nu_2-m} &= \pi\frac{\cos\left[\Gamma_1^2-\Gamma_2^2-\nu_1 b_1+\nu_2 b_2+\pi\delta\right]}{\sin(\pi\delta)}. \end{aligned} \tag{A11}$$

We can express these as functions of the variable $\alpha_i$ defined in Eq. (14),

$$\begin{aligned} \sum_m\frac{\cos C_1}{\nu_1-m} &= \pi\frac{\cos[\alpha_1+\alpha_2]}{\sin(\pi\delta)}, \\ \sum_m\frac{\cos C_2}{\nu_1-m} &= \pi\frac{\cos[\alpha_2-\alpha_1+\pi\delta]}{\sin(\pi\delta)}, \\ \sum_m\frac{\cos D_1}{\nu_2-m} &= \pi\frac{\cos[\alpha_1+\alpha_2]}{\sin(\pi\delta)}, \\ \sum_m\frac{\cos D_2}{\nu_2-m} &= \pi\frac{\cos[\alpha_2-\alpha_1+\pi\delta]}{\sin(\pi\delta)}. \end{aligned} \tag{A12}$$

Under the assumption that $\nu_1,\nu_2 \gg 1$ such that $\nu_1 \sim \nu_2$, we can use these expressions along with (A7) to express (A2)

as

$$\frac{1}{\rho}\frac{\partial S_6(\rho)}{\partial \rho} = -\frac{\nu_1(\Gamma_1\Gamma_2)^{-1}}{2\sin(\pi\delta)\rho^4}\left[\left(\Gamma_1^2+\Gamma_2^2\right)^2\cos(\alpha_1+\alpha_2)\right.$$
$$\left.+\left(\Gamma_2^2-\Gamma_1^2\right)^2\cos(\alpha_2-\alpha_1+\pi\delta)\right]. \quad \text{(A13)}$$

We now make the simplifying assumption, valid for small $\delta$, that $\cos(\alpha_2-\alpha_1)\approx\cos(\alpha_2-\alpha_1+\pi\delta)$. Through the addition and sum trigonometric identities, this assumption permits us to write

$$\frac{1}{\rho}\frac{\partial S_6(\rho)}{\partial \rho} = -\frac{\nu_1(\Gamma_1\Gamma_2)^{-1}}{\sin(\pi\delta)\rho^4}\left[\left(\Gamma_1^4+\Gamma_2^4\right)\cos\alpha_1\cos\alpha_2\right.$$
$$\left.-2\Gamma_1^2\Gamma_2^2\sin\alpha_1\sin\alpha_2\right]. \quad \text{(A14)}$$

We can follow the same SEW expansion procedure outlined above to find the single-wave contributions to Eq. (11),

$$\frac{1}{\rho}\frac{\partial S_1^{\nu_i}(\rho)}{\partial \rho} = -\frac{\nu_1}{\sin(\delta\pi)\rho^4}\Gamma_i^2(\cos^2\alpha_i-\sin^2\alpha_i). \quad \text{(A15)}$$

This expression along with that in (A13) allows us to write Eq. (11) in the factored form

$$F(\varepsilon,\nu_1,\nu_2) = \frac{\nu_1^2}{\sin(\pi\delta)\rho^4}\left[(\varepsilon_1\Gamma_1\sin\alpha_1+\varepsilon_2\Gamma_2\sin\alpha_2)^2\right.$$
$$-(\varepsilon_1\Gamma_1\cos\alpha_1)^2-(\varepsilon_2\Gamma_2\cos\alpha_2)^2$$
$$\left.-\varepsilon_1\varepsilon_2\frac{\left(\Gamma_1^4+\Gamma_2^4\right)}{\Gamma_1\Gamma_2}\cos\alpha_1\cos\alpha_2\right]. \quad \text{(A16)}$$

Finally, in order to avoid the singularity at $\kappa_i\rho=\nu_i$, facilitate comparison to previous SEW results [4], and lay the groundwork for examining the $\rho<\nu_i/\kappa_i$ limit, we make the substitution that is valid for $\kappa_i\rho>\nu_i+(\frac{1}{2}\nu_i)^{1/3}$ that

$$\left(\frac{2}{\pi}\right)^{1/2}\frac{\left[(\kappa_i\rho)^2-\nu_i^2\right]^{1/4}}{\rho}\to\left|H_{\nu_i}^{1'}(\kappa_i\rho)\right|, \quad \text{(A17)}$$

where the derivative of the Hankel function is with respect to $\rho$. Substituting this result into the expression for $F$, we recover the result shown in Eq. (13).

## APPENDIX B

In order to simplify the second term of Eq. (13), we examine the remaining cross-term,

$$\varepsilon_1\varepsilon_2\frac{\left[A_1^4(\rho)+A_2^4(\rho)\right]}{A_1(\rho)A_2(\rho)}\cos\alpha_1\cos\alpha_2. \quad \text{(B1)}$$

We rewrite this as

$$\varepsilon_1\varepsilon_2A_1A_2\left[\left(\frac{A_1}{A_2}\right)^2+\left(\frac{A_2}{A_1}\right)^2\right]\cos\alpha_1\cos\alpha_2. \quad \text{(B2)}$$

Using the forms of $A_1, A_2$ from Appendix A, we can write the ratio

$$\frac{A_1}{A_2}=\left[\frac{(\kappa_1\rho)^2-\nu_1^2}{(\kappa_2\rho)^2-\nu_2^2}\right]^{1/2}. \quad \text{(B3)}$$

For the large $\rho\kappa_i\gg\nu_i$ case, we see that this ratio approaches

$$\frac{A_1}{A_2}\approx\frac{\kappa_1}{\kappa_2}. \quad \text{(B4)}$$

Therefore, we see that in the event that the ratio of the wave numbers is on the order of unity $\kappa_1/\kappa_2\sim1$, we can express the cross-term from (B1) as

$$2\varepsilon_1\varepsilon_2A_1A_2\cos\alpha_1\cos\alpha_2. \quad \text{(B5)}$$

This allows us to factor the terms in Eq. (13) to yield the simplified form Eq. (17).


[1] R. Davidson, *Methods in Nonlinear Plasma Theory* (Academic Press, New York, 1972).
[2] R. Sagdeev and A. Galeev, *Nonlinear Plasma Theory*, Frontiers in Physics (W. A. Benjamin, New York, 1969).
[3] C. Karney and A. Bers, Phys. Rev. Lett **39**, 550 (1977).
[4] C. Karney, Phys. Fluids **21**, 1584 (1978).
[5] D. Bénisti, A. K. Ram, and A. Bers, Phys. Lett. A **233**, 209 (1997).
[6] P. Chia, L. Schmitz, and R. Conn, Phys. Plasmas **3**, 1545 (1996).
[7] A. K. Ram, A. Bers, and D. Benisti, J. Geophys. Res. **103**, 9431 (1998).
[8] D. Bénisti, A. K. Ram, and A. Bers, Phys. Plasmas **5**, 3224 (1998).
[9] D. Bénisti, A. K. Ram, and A. Bers, Phys. Plasmas **5**, 3233 (1998).
[10] D. J. Strozzi, A. K. Ram, and A. Bers, Phys. Plasmas **10**, 2722 (2003).
[11] R. Spektor and E. Y. Choueiri, Phys. Rev. E **69**, 046402 (2004).
[12] Z.-M. Sheng, L. Yu, G. Hao, and R. White, Phys. Plasmas **16**, 072106 (2009).
[13] B. Jorns and E. Y. Choueiri, Phys. Rev. Lett. **106**, 085002 (2011).
[14] A. Lichtenberg and M. Lieberman, *Regular and Chaotic Dynamics*, Applied Mathematical Sciences Vol. 38 (Springer-Verlag, Berlin, 1992).
[15] H. Goldstein, *Classical Mechanics* (Addison-Wesley, Cambridge, MA, 1951).
[16] B. V. Chirikov, Phys. Rep. **52**, 263 (1979).
[17] M. Sandri, Math. J. **6**, 78 (1996).
[18] H. Fukyama, R. I. Momota, Tatani, and T. Takizuka, Phys. Rev. Lett. **38**, 701 (1977).
[19] M. Abramowitz and I. Stegun, *Handbook of Mathematical Functions: With Formulas, Graphs, and Mathematical Tables*, Applied Mathematics Series Vol. 55 (Dover, London, 1964).
[20] T. Stix, *Waves in Plasmas* (American Institute of Physics, New York, 1992).
[21] F. Skiff, F. Anderegg, and M. Q. Tran, Phys. Rev. Lett. **58**, 1430 (1987).
[22] A. Fasoli, F. Skiff, R. Kleiber, M. Q. Tran, and P. J. Paris, Phys. Rev. Lett. **70**, 303 (1993).